Oncogene (2010) 29, 3276–3286

www.nature.com/onc

ORIGINAL ARTICLE

Bortezomib decreases Rb phosphorylation and induces caspase-dependent apoptosis in Imatinib-sensitive and -resistant Bcr-Abl1-expressing cells

MP Albero[1], JM Vaquer[1], EJ Andreu[2], JJ Villanueva[1], L Franch[1], C Ivorra[1], E Poch[1], X Agirre[2], F Prosper[2] and I Pérez-Roger[1]

[1]*Department of Chemistry, Biochemistry and Molecular Biology, Cardenal Herrera-CEU University, Moncada, Spain and* [2]*Hematology Department and Area of Cell Therapy, Clinica Universidad de Navarra, Foundation for Applied Medical Research University of Navarra, Pamplona, Spain*

The use of *c-abl*-specific inhibitors such as Imatinib (IM) or Dasatinib has revolutionized the treatment of chronic myeloid leukemia (CML). However, a significant percentage of patients become resistant to IM. In this report, we have analyzed the possibility of using the proteasome as a molecular target in CML. Our results show that cells that express Bcr-Abl1 are more sensitive to the inhibition of the proteasome with Bortezomib (Btz) than control cells. This treatment reduces the proliferation of Bcr-Abl1-expressing cells, by inactivating NF-κB2 and decreasing the phosphorylation of Rb, eventually leading to an increase in caspase-dependent apoptosis. Furthermore, we show that Btz also induces cell-cycle arrest and apoptosis in cells expressing Bcr-Abl1 mutants that are resistant to IM. These results unravel a new molecular target of Btz, that is the Rb pathway, and open new possibilities in the treatment of CML especially for patients that become resistant to IM because of the presence of the T315I mutation.
Oncogene (2010) **29,** 3276–3286; doi:10.1038/onc.2010.81; published online 22 March 2010

Keywords: Bortezomib; CML; Bcr-Abl1; Imatinib resistance; Rb; apoptosis

Introduction

Chronic myeloid leukemia (CML) appears as a consequence of the reciprocal translocation between chromosomes 9 and 22, giving rise to the expression of the Bcr-Abl1 oncoprotein. Current treatment of the disease includes the use of the specific tyrosine-kinase inhibitor Imatinib (IM). Even though treatment with IM induces complete cytogenetic remission in >70% of CML patients, the appearance of Bcr-Abl1 mutants resistant to IM remains a significant problem (Druker, 2008). This resistance arises mainly by point mutations in the ATP-binding pocket at the active site of the tyrosine-kinase Abl, which reduces the affinity for IM without changing the affinity for ATP (Shah and Sawyers, 2003). Second generation inhibitors, such as Dasatinib and Nilotinib, have been proven efficient against most Bcr-Abl1 mutants, but the T315I mutant remains insensitive to the new inhibitors (Ramirez and DiPersio, 2008).

We have earlier reported that Bcr-Abl1 induces the degradation of the cell-cycle inhibitor p27Kip1 by the proteasome, through the induction of the F-box protein Skp2 (Andreu *et al*., 2005). These results prompted us to explore the possibility of using the proteasome as a potential therapeutic target in the treatment of CML. The use of the proteasome inhibitor Bortezomib (Btz) has been successful in the treatment of multiple myeloma and mantle cell lymphoma (Chauhan *et al*., 2008; Wei and Roberts, 2008). Recently, it has also been shown that Bcr-Abl1 induces the activity of the proteasome, again supporting the idea of using the proteasome as a suitable target in Bcr-Abl1-expressing cells (Crawford *et al*., 2009).

In this report, we have analyzed the effect of Btz on proliferation and survival of different cells expressing Bcr-Abl1, such as the murine BaF/3 cell line stably transduced with Bcr-Abl1, the human blast crisis-derived TCC-S cell line, and primary CD34+ cells from CML patients. We have also used BaF/3 cells expressing mutant forms of Bcr-Abl1 that confer resistance to IM, including the highly resistant T315I mutant. Our results show that Bcr-Abl1-expressing cells, including the IM-resistant ones, are more sensitive to Btz than control cells and that Btz treatment reduces proliferation and induces caspase-dependent apoptosis. We have also analyzed the molecular mechanisms responsible for the effect of Btz in these cells. Our results underscore the effect of Btz on the Rb pathway of cell-cycle control and support the use of Btz in the treatment of CML, particularly for those patients that become resistant to IM as a consequence to the T315I mutation.

Results

Btz inhibits proliferation of Bcr-Abl1-expressing cells

To test the possibility of using the proteasome as a therapeutic target in the treatment of CML, we treated

Correspondence: Dr I Pérez-Roger, Department of Chemistry, Biochemistry and Molecular Biology, Cardenal Herrera-CEU University, Edif. Seminario, Av Seminario, Moncada, Valencia 46113, Spain.
E-mail: iperez@uch.ceu.es
Received 10 April 2009; revised 25 January 2010; accepted 4 February 2010; published online 22 March 2010

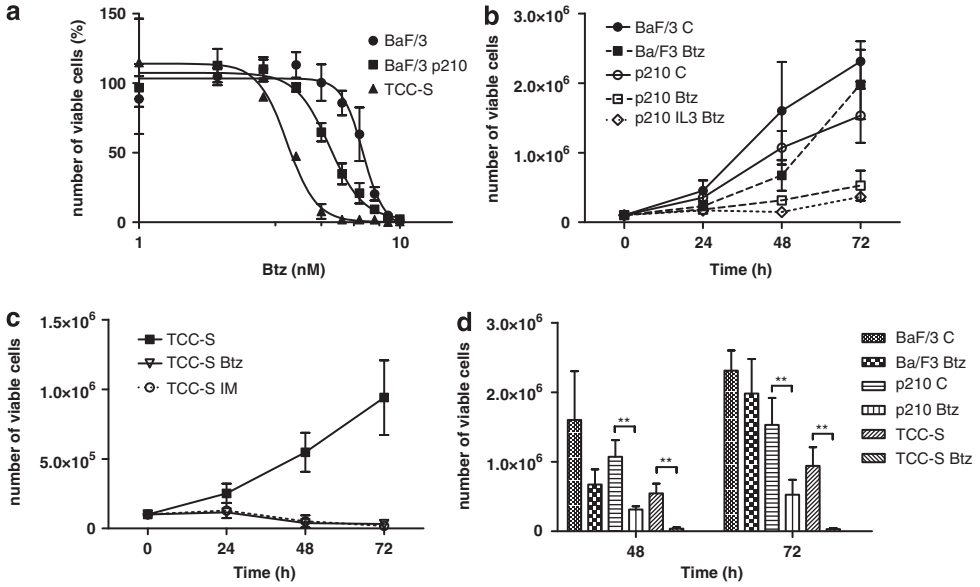

Figure 1 Btz inhibits proliferation of Bcr-Abl1-expressing cells. (**a**) Dose response of Btz on BaF/3, BaF/3-p210, and TCC-S cell lines. Cells were seeded at a density of 1×10^5/ml and treated with a single dose of Btz ranging from 0 to 10 nM. Viable cell counts at 72 h were used to plot the dose-response effect. Cell counts relative to control (100%) from four different experiments are represented as mean ± s.d. Differences between BaF/3 and BaF/3-p210 cells are statistically significant at 5, 6, and 7 nM, as revealed by a one-way analysis of variance followed by a Tukey's multiple comparison test ($P<0.01$). Note that the maximal difference between BaF/3 and BaF/3-p210 is at 6 nM Btz. (**b**) Effect of Btz on the proliferation of BaF/3 and BaF/3-p210. Growth of untreated (C) and Btz-treated (6 nM, Btz) cells was followed by viable cell count every 24 h. Mean ± s.d. from four different experiments is shown. Addition of 10% WEHI-conditioned medium to the culture medium of BaF/3-p210 cells as a source of murine IL-3 (p210 IL3 Btz) does not prevent the effect of Btz on these cells. (**c**) The effect of 6 nM Btz is similar to that of 0.3 μM IM on the human-derived TCC-S cell line. Cells were treated and counted as in (**b**). The dose of 0.3 μM IM was selected from an earlier dose-response experiment (not shown). (**d**) Differences between untreated (C) and Btz-treated (Btz) cells from (**b**) and (**c**) at 48 and 72 h are plotted as columns (mean + s.d.). Student's *t*-test analysis revealed statistically significant differences between Btz and C at 48 and 72 h only in Bcr-Abl1-expressing cells, but not in BaF/3 cells (**$P<0.01$).

control BaF/3 cells and BaF/3 cells that stably express wt Bcr-Abl1 p210 (BaF/3-p210) with different doses of the proteasome inhibitor Btz, ranging from 0 to 100 nM. Btz is lethal above 10 nM on both cell lines (not shown). The dose-response analysis between 0 and 10 nM Btz reveals that the Bcr-Abl1-expressing BaF/3 cells are more sensitive to Btz than the parental BaF/3 cells (Figure 1a). The difference between BaF/3-p210 and control BaF/3 cells is statistically significant ($P<0.05$) at 5, 6, and 7 nM Btz. The IC_{50} values are 6.2 and 4.7 nM at 48 h and 7.2 and 5.3 nM at 72 h for BaF/3 and BaF/3-p210 cells, respectively. As the maximal difference between BaF/3 and BaF/3-p210 at 72 h is seen with the dose of 6 nM, this is the dose we decided to use for the rest of the experiments.

We also wanted to analyze the sensitivity of human cells to Btz. We chose the TCC-S cell line, which has been earlier used as a model of Ph+ cells (Kano *et al*., 2007; Roman-Gomez *et al*., 2007). These cells derive from a CML patient in blast crisis and express mainly the p210 form of Bcr-Abl1. This cell line is more sensitive than the other two cell lines tested, with IC_{50} values of 2.8 nM at 48 h and 3.7 nM at 72 h (Figure 1a).

We then compared the effect of a 6-nM dose of Btz on the growth curve of BaF/3 and BaF/3-p210 cells. As shown in Figure 1b, Btz treatment initially reduces the proliferation of control BaF/3 cells at 24–48 h, but they recover in the 48–72 h period. However, Bcr-Abl1-expressing BaF/3 cells show a permanent growth arrest for the length of the experiment. The smaller effect of Btz on BaF/3 compared with BaF/3-p210 cells could be due to the fact that control cells are cultured in the presence of IL3. However, when we add IL3 to the BaF/3-p210 cells, the effect of Btz is indistinguishable from that shown in the absence of IL3 (Figure 1b). Therefore, the sensitivity to Btz is not a consequence of the different culture conditions, but most likely because of the expression of Bcr-Abl1. In the case of the TCC-S cell line, we compared the effect of Btz with that of IM. First, we calculated the IC_{50} of IM for this cell line, getting a value of 0.2 μM (not shown). Figure 1c shows that the treatment with 6 nM Btz causes the same growth inhibition as the treatment with 0.3 μM IM. The difference between untreated and Btz-treated cells is statistically significant ($P<0.01$) both at 48 and 72 h in the BaF/3-p210 and TCC-S cell lines, but not in the parental BaF/3 cell line (Figure 1d). These results show that Bcr-Abl1-expressing cells are more sensitive to Btz treatment than control cells.

We then explored the possible synergy between Btz and IM. We used a fix ratio of doses ranging from 1 to 5 nM Btz and from 0.1 to 0.5 μM IM, around the IC_{50} for each one of them in the BaF/3-p210 cell line. The combination index obtained using the Chou–Talalay method indicates that there is an additive effect of both drugs, but no synergism, at least under our experimental

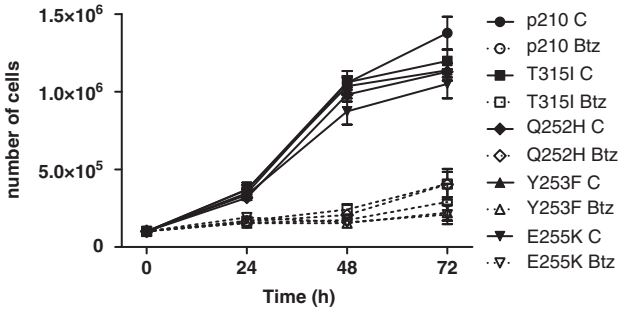

Figure 2 Btz inhibits proliferation of cells expressing Bcr-Abl1 mutants that confer resistance to IM. BaF/3-expressing wt Bcr-Abl1 (p210), or different mutants of the protein (T315I, Q252H, Y253F, and E255K) untreated (C) or treated with 6 nM Btz (Btz) were seeded and counted as in Figure 1. Mean ± s.e.m. is represented from a total of eight different experiments. There are no statistical differences among control cells or among treated cells, but in each cell line, the difference between treated and untreated is significant, as revealed by a one-way analysis of variance followed by a Tukey's multiple comparison test ($P<0.01$).

conditions (data not shown). As IM and Btz have additive effects, this would suggest that the activation of the proteasome in Bcr-Abl1-expressing cells is a consequence of Bcr-Abl1-kinase activity.

IM-resistant Bcr-Abl1-expressing cells are also sensitive to Btz

To see whether Btz could have an effect on cells expressing IM-resistant forms of Bcr-Abl1, we used BaF/3 cells expressing four different mutants of Bcr-Abl1: T315I, Q252H, Y253F, and E255K. Q252H is only partially resistant to IM and is affected by the drug at high doses. The highly resistant T315I mutation affects the direct contact between IM and Bcr-Abl1, therefore, preventing this interaction (Shah and Sawyers, 2003). We cultured these cell lines in parallel with the one expressing wt Bcr-Abl1 (BaF/3-p210) and treated them with a single 6 nM dose of Btz. As shown in Figure 2, Btz inhibits proliferation of all these Bcr-Abl1-expressing cell lines to the same extent, indicating that Btz is equally effective against IM-sensitive and -resistant Bcr-Abl1-expressing cells. One-way analysis of variance followed by Tukey's analysis revealed that all the mutant cell lines behave the same as the BaF/3-p210 one, and that there are statistically significant differences between untreated and treated groups at 48 and 72 h ($P<0.01$).

Btz inhibits S-phase entry in Bcr-Abl1-expressing cells

We then wanted to characterize the effect of Btz on the cell cycle of these cells. DNA profiles of BaF/3 control and BaF/3-p210 cells show that 48 h after the addition of Btz, there is an accumulation of the Bcr-Abl1-expressing cells in the G0/G1 phase of the cell cycle, whereas control cells are minimally affected (Figure 3a). We also analyzed the cell-cycle profile of mutant Bcr-Abl1-expressing cells (Figure 3a). In all cases, there is a reduction of the proliferating populations (S + G2/M) and an accumulation of cells in G0/G1. The DNA profiles also show that Btz induces cell death, as there is an increase in the sub-G0/G1 population.

To characterize the nature of the cell-cycle arrest in more detail and quantify the percentage of cells in each of the cell-cycle phases more precisely, we performed an 5-ethynyl-2′-deoxyuridine (EdU) incorporation assay. Figure 3b shows an example of this analysis with BaF/3 and BaF/3-p210 cells. In BaF/3 cells, there is a slight reduction of the S-phase population at 24 h, but the cells have recovered at 48 h after the addition of Btz. In contrast, there is a big decrease of the S-phase population in the BaF/3-p210 cells that is permanent. Quantification of the EdU incorporation experiments (Figure 3c) reveals that 48 h after Btz addition, the cell-cycle profile of control BaF/3 cells is not statistically different from untreated cells. In contrast, all the cell lines expressing Bcr-Abl1, including the mutant forms that are IM resistant, display a G0/G1 arrest when treated with Btz. The differences between Btz-treated cells and the untreated controls are statistically significant in the G0/G1 accumulation ($P<0.05$ in all cases) and also in the S-phase reduction ($P<0.01$ in all cases).

Btz treatment reduces the phosphorylation and the activity of Rb in Bcr-Abl1-expressing cells

At the molecular level, Rb phosphorylation regulates the transition from G1 into S phase (Khidr and Chen, 2006). Therefore, we analyzed the effect of Btz on the phosphorylation status of Rb by western blot. As shown in Figure 4a, Btz treatment causes a reduction in the total level of Rb protein, both in BaF/3 and in BaF/3-p210 cells. However, in the case of the BaF/3-p210 and not the BaF/3 cells, a faster migrating band, corresponding to the hypo-phosphorylated form of Rb (Rb), can be detected. At the same time, there is a decrease in the intensity of the slower migrating bands, corresponding to hyper-phosphorylated Rb (P-Rb). This change in the phosphorylation status of Rb can be detected as early as 12 h and is more evident at 24 h (Figure 4a). If we represent the ratio between the hypo-phosphorylated and the hyper-phosphorylated forms of the protein (Rb/P-Rb), the increase in this ratio is statistically significant at 12 and 24 h after Btz addition compared with time 0 h ($P<0.05$; Figure 4c). We compared this effect with that of the Bcr-Abl1-kinase inhibitor IM. As earlier reported (Andreu *et al*., 2005), IM also increases the level of hypo-phosphorylated Rb, finally inducing the disappearance of the hyper-phosphorylated forms of the protein (Figure 4a).

Rb regulates the expression of cyclins such as cyclin A (CycA), through the E2F family of transcription factors. Therefore, the expression of CycA reflects the activity of Rb. As shown in Figure 4a, the amount of CycA protein decreases as the levels of P-Rb also decrease upon Btz or IM treatment, confirming that the effect of these drugs on Rb is also functional. Rb phosphorylation is mediated by Cyclin/Cdk complexes active during G1 (Murray, 2004). The activity of these complexes is in

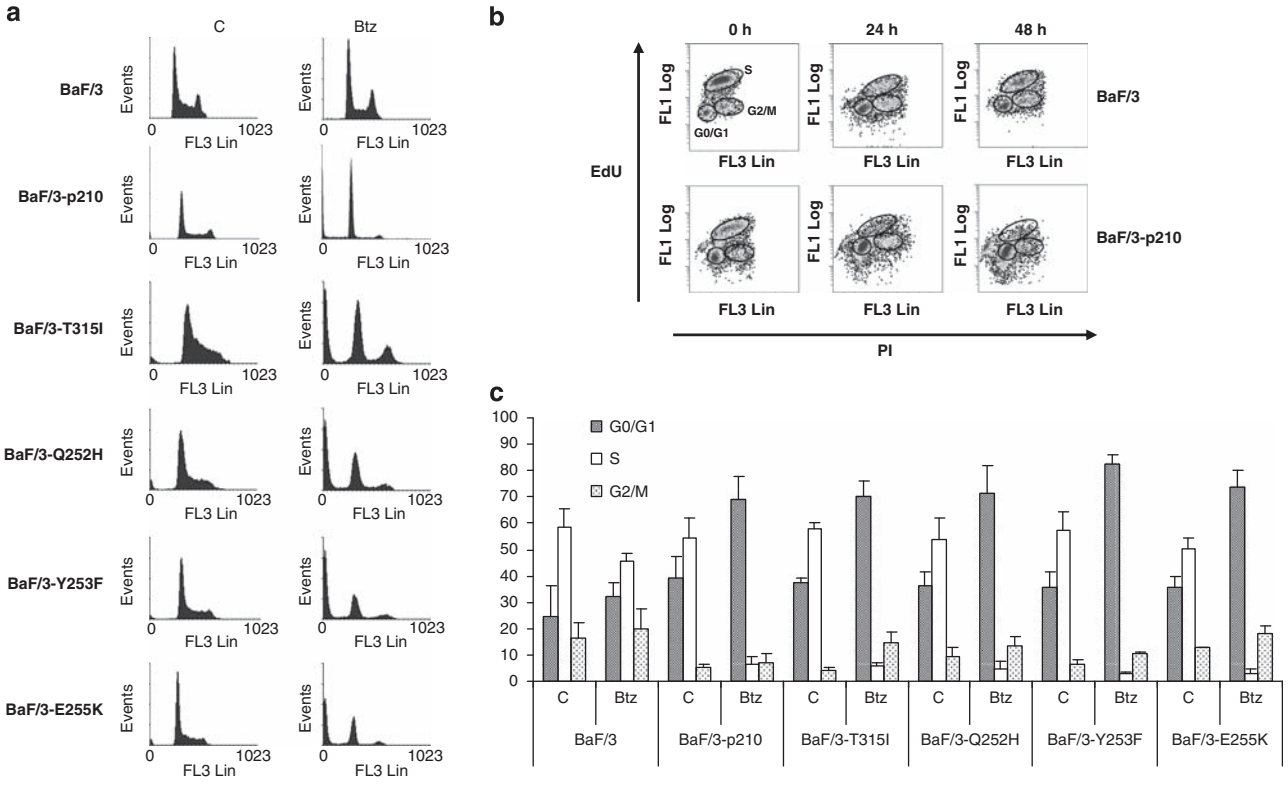

Figure 3 Btz induces a G1 cell-cycle arrest in Bcr-Abl1-expressing cells. (**a**) BaF/3 cells and derivatives expressing wt Bcr-Abl1 (p210) and different IM resistant mutants (T315I, Q252H, Y253, and E255K), untreated (C, left) or treated with 6 nM Btz (Btz, right) for 48 h were fixed, stained with PI, and analyzed by flow cytometry as described in Materials and methods. The experiment shown is a representative example from six different experiments. (**b**) and (**c**) To quantify the different cell-cycle populations in each case, cells received a 30-min pulse of the nucleotide analog EdU. EdU/PI double staining allows for an accurate quantification of cells in G0/G1, S, and G2/M. An example of this kind of analysis for BaF/3 and BaF/3-p210 cells at 0, 24, and 48 h after the addition of 6 nM Btz is shown in (**b**). Quantification of such experiments ($n=3$) with BaF/3, BaF/3-p210, and the IM-resistant Bcr-Abl1-expressing BaF/3 cells at 48 h is represented in (**c**) as mean + s.d. There are no significant differences between C and Btz-treated BaF/3 cells (the G0/G1–S–G2/M values are 24 ± 11–58 ± 7–16 ± 5 for untreated cells and 32 ± 4–45 ± 2–20 ± 7 for Btz-treated cells). In all other cases, Student's *t*-test reveals that there are statistically significant differences indicating an increase in G0/G1 ($P<0.05$) and a decrease in S phase ($P<0.01$) in Btz-treated cells compared with each control (as an example, for the BaF/3-p210 cells, the G0/G1 – S – G2/M values are 39 ± 7–54 ± 7–5.4 ± 0.8 for untreated cells and 68 ± 9–6 ± 2–7 ± 3 for Btz-treated cells).

turn negatively regulated by inhibitors of the Cip/Kip family, such as p21Cip1 (p21) and p27Kip1 (p27) (Sherr and Roberts, 2004). As shown in Figure 4a, Btz treatment results in the accumulation of both cell-cycle inhibitors. p21 accumulates both in control and Bcr-Abl1-expressing cells. However, in BaF/3 cells, there is only a slight accumulation of p27 at 12 h and not later on, whereas in BaF/3-p210 cells, p27 accumulation increases with time. In contrast, IM treatment only induces the accumulation of p27 and causes a reduction in p21 expression.

In the case of IM-resistant Bcr-Abl1-expressing BaF/3 cells, Btz not only induces a decrease in the level of total Rb, but also of P-RB (Figure 4b). In fact, the increase of the Rb/P-RB ratio is higher than the decrease of total Rb (Figure 4c). In every case, the P-Rb decrease is detected at 12 h and the effect is more evident at 24 h (Figures 4b and c). Similar to the BaF/3-p210 cells, the mutant Bcr-Abl1-expressing cell lines also display a decrease in CycA expression and an increase in p21 and p27 protein levels (Figure 4b). Therefore, the effect of Btz at the molecular level on the cell-cycle regulatory machinery of cells expressing Bcr-Abl1 is the same regardless to the IM sensitivity of the cells.

Btz prevents the activation of NF-κB

One of the known targets of Btz in different models is the transcription factor NF-κB (Galimberti *et al*., 2008). We assayed the effect of Btz on the activity of this protein by electrophoretic mobility shift assay and found that Btz reduces the DNA-binding activity of NF-κB on BaF/3 and Ba/F3-p210 cells with no significant differences between both cell types (Figure 5a). Therefore, the activity of this transcription factor does not seem to be responsible for the cell-cycle arrest that we see only in BaF/3-p210 cells. As the initial level of NF-κB activity is higher in BaF/3-p210 cells, we cannot rule out the possibility that the disappearance of NF-κB activity has a bigger impact on these cells. There are two alternative pathways of NF-κB activation: the canonical and the non-canonical pathways (Pomerantz and Baltimore, 2002). The second one involves the proteasome-dependent activation of NF-κB2 from a 100

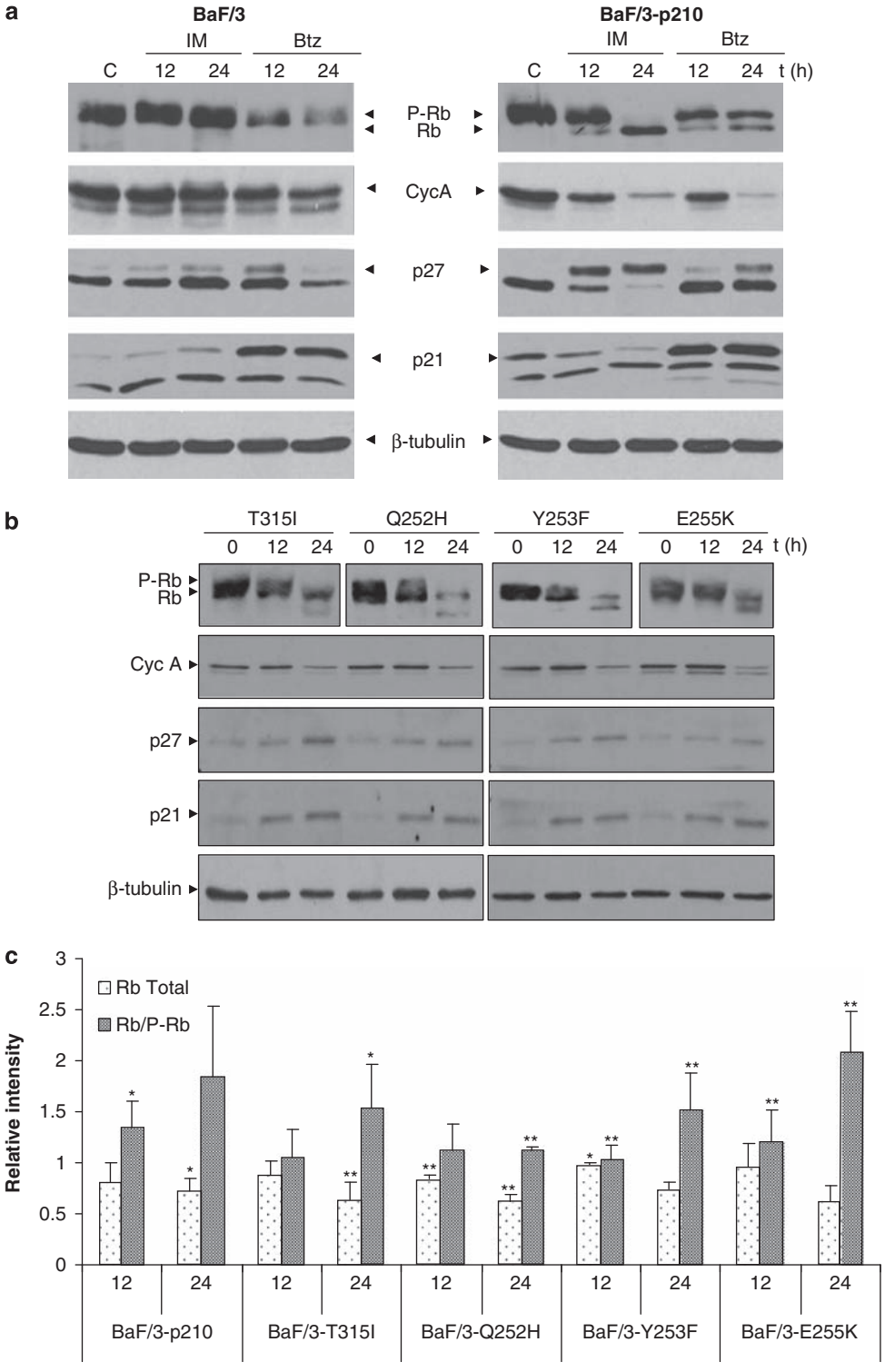

Figure 4 Btz treatment decreases the phosphorylation and the function of Rb in Bcr-Abl1-expressing cells. (**a**) Control BaF/3 (left) and Bcr-Abl1-expressing BaF/3-p210 (right) cells were treated with 2 μM IM or 6 nM Btz for 12 and 24 h or untreated (C) and cell extracts were prepared and analyzed by western blot with the appropriate primary antibodies, as indicated. In the Rb blot (top), the faster migrating band corresponds to the hypo-phosphorylated form of Rb (Rb), whereas the slower migrating bands correspond to the hyper-phosphorylated forms of the protein (P-Rb). β-tubulin is used as a loading control. Shown is a representative blot of three independent experiments. (**b**) Similar analysis as in (**a**) was performed with extracts from untreated (C) and treated with 6 nM Btz for 12 and 24 h BaF/3 cells expressing four different Bcr-Abl1 mutants that confer IM resistance. A single band is detected in the p27 blot because a different antibody was used that does not detect the lower band seen in (**a**). (**c**) Btz treatment reduces the amount of total Rb as well as its phosphorylation. P-Rb and total Rb bands were quantified using the QuantityOne software (Bio-Rad). Columns represent mean + s.d. relative to the values at $t = 0$ (value of 1) from three independent experiments as the ones shown in (**a**, **b**). Both total Rb and the Rb/P-RB ratio are represented. Student's *t*-test reveals that the differences between Btz and control cells are significant as early as 12 h in most cases (*$P < 0.05$; **$P < 0.01$).

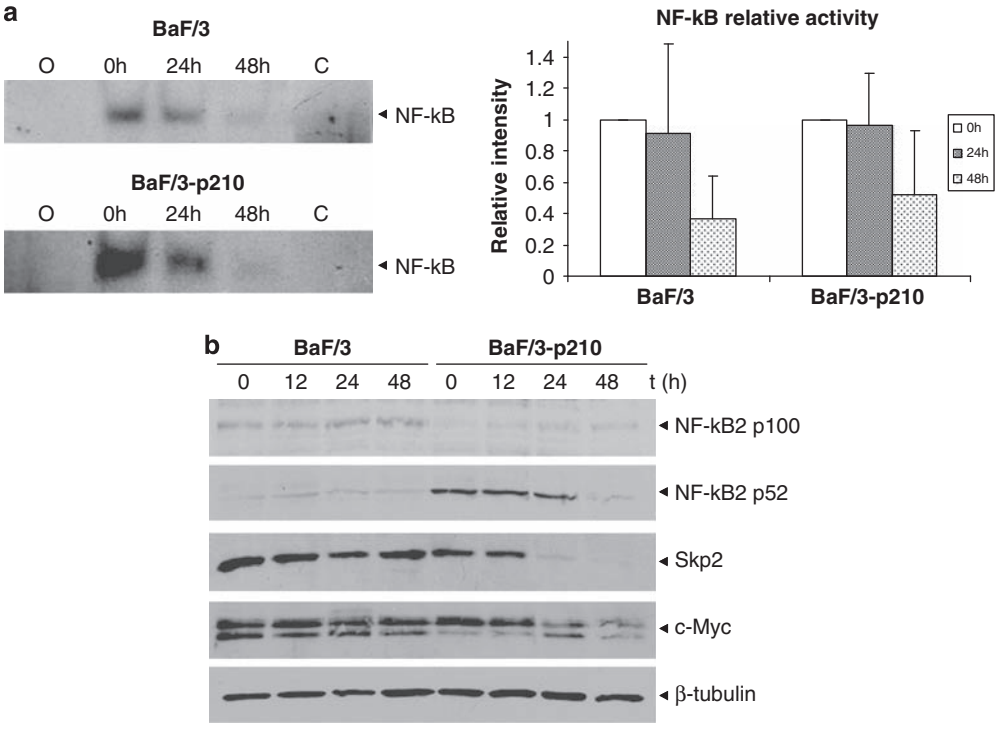

Figure 5 Btz inhibits the activation of NF-κB2 in Bcr-Abl1-expressing cells. (**a**) A digoxigenin-labeled double-stranded DNA oligonucleotide with the consensus sequence for NF-κB was incubated with nuclear extracts from control BaF/3 (top) and Bcr-Abl1-expressing BaF/3-p210 (bottom) cells treated with 6 nM Btz for the times indicated. The DNA-binding activity of NF-κB in those extracts was analyzed by electrophoretic mobility shift assay. O: labeled oligonucleotide without extract. C: binding was competed with a 50-fold molar excess of unlabeled oligonucleotide. The graph on the right shows the quantification of five independent assays as the one shown on the left. Columns represent the mean + s.d. of the intensity of the bands relative to time 0 h. (**b**) BaF/3 and BaF/3-p210 cells were treated with 6 nM Btz for the indicated times and cell extracts were prepared and analyzed by western blot with the indicated antibodies. The antibody against NF-κB2 recognizes both the 100 kDa (inactive) and the 52 kDa (active) forms of the protein. β-tubulin is used as a loading control. A representative blot of three different experiments is shown.

to 52 kDa form (Heusch *et al*., 1999). As Btz could be affecting this activation, we analyzed the processing and activation of NF-κB2 in our experimental system by western blot. As shown in Figure 5b, BaF/3-p210 cells exhibit a higher level of processed, active p52-NF-κB2 protein than BaF/3 control cells. However, on Btz treatment, there is a marked reduction in the level of the 52-kDa active form of NF-κB2.

It has been shown that the NF-κB2 subunit is relevant for the regulation of Skp2 and c-Myc expression (Barre and Perkins, 2007). It is known that these two proteins are among the many factors that regulate the levels and activity of the cell-cycle inhibitors p21Cip1 and p27Kip1 (Perez-Roger *et al*., 1999; Kossatz *et al*., 2004). On the other hand, Bcr-Abl1-kinase activity inhibition with IM results in the downregulation of both Skp2 and c-Myc, indicating that these two proteins are molecular targets of Bcr-Abl1 (Sawyers, 1993; Andreu *et al*., 2005). Therefore, we analyzed the effect of Btz on Skp2 and c-Myc and found that both show lower levels in Btz-treated cells expressing Bcr-Abl1, with no significant change in BaF/3 control cells (Figure 5b).

Btz induces caspase-dependent apoptosis of Bcr-Abl1-expressing cells

Treatment with Btz in different tumor models induces apoptosis *in vitro* (Brignole *et al*., 2006; Perez-Galan *et al*., 2006; Stapnes *et al*., 2007; Strauss *et al*., 2007; Galimberti *et al*., 2008; Zhao *et al*., 2008). As noted earlier, Btz induces an increase of the sub-G0/G1 population (Figure 3a). To evaluate the effect of Btz on the survival of Bcr-Abl1-expressing cells, we double stained the cells with Annexin-V and propidium iodide (PI) to distinguish between apoptosis and necrosis and analyzed them by flow cytometry. The results shown in Figure 6a indicate that Btz treatment induces apoptosis in Bcr-Abl1-expressing cells, as indicated by the increase in the Annexin V positive population. In the case of BaF/3 cells, there is an initial increase in the apoptotic population at 24 h, but then it decreases at 48 and 72 h. The difference between BaF/3-p210 and control BaF/3 cells is statistically significant at 48 and 72 h ($P<0.01$). To test the caspase dependency of the apoptosis induced by Btz in our model, we used the pan-caspase inhibitor z-VAD and analyzed apoptosis by measuring the appearance of the sub-G0/G1 apoptotic population in the DNA profile (Figure 6b). Pre-treatment of the cells with this inhibitor partially abrogates the cell death induced by Btz, suggesting that caspase activation is at least in part necessary for the induction of apoptosis by Btz. In the IM-resistant Bcr-Abl1-expressing cells, Btz also induces apoptosis and it can be partially prevented by z-VAD pre-treatment (Figure 6b). Quantification of the sub-G0/G1 apoptotic population gives a statistically

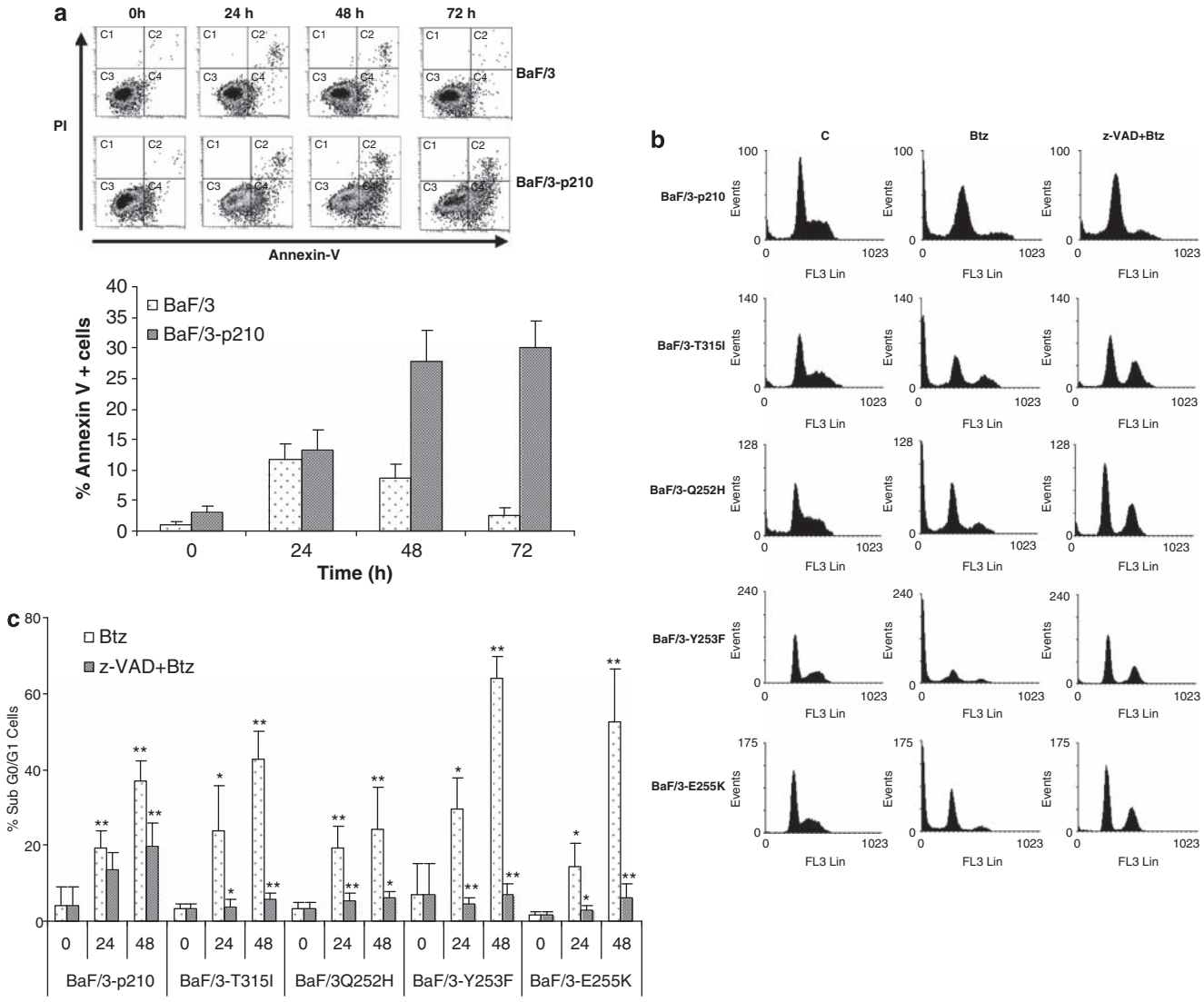

Figure 6 Btz induces caspase-dependent apoptosis in Bcr-Abl1-expressing cells. (**a**) Control BaF/3 (top row) and Bcr-Abl1-expressing BaF/3-p210 (low row) cells were treated with 6 nM Btz for 0, 24, 48, and 72 h and stained with Annexin-V and PI. Flow cytometry analysis reveals viable cells (negative for Annexin-V and PI staining, bottom left square) early apoptotic (Annexin-V positive, bottom right square) and late apoptotic-necrotic (Annexin-V and PI positive, top-right square) cell populations. Bottom: Quantification of the apoptotic, Annexin-V positive populations from three different experiments as the one shown above reveals that Btz induces more apoptosis in Bcr-Abl1-expressing cells than in control BaF/3 cells at 48 and 72 h ($P<0.01$). (**b**) BaF/3 cells expressing wt and mutant forms of Bcr-Abl1 were untreated (C), treated with 6 nM Btz (Btz), or pre-treated with z-VAD for 1 h before the addition of Btz; 48 h later, cells were stained with PI to analyze and quantify the apoptotic sub-G0/G1 population. The quantification of three different such experiments is shown in (**c**), showing that Btz induces apoptosis at 24 and 48 h compared with untreated controls and that z-VAD reduces this apoptosis also at 24 and 48 h compared with the Btz column for each cell line (*$P<0.05$; **$P<0.01$).

significant difference at 24 and 48 h after Btz treatment compared with time 0 h in all cell lines. In addition, the anti-apoptotic effect of z-VAD is significant in all cases (Figure 6c).

Finally, we tested whether Btz could have an effect on primary CD34+ cells from a CML patient. As a control, we used primary non-CML CD34+ cells from umbilical cord. We treated the cells with 6 and 10 nM Btz and analyzed the cell-cycle profile by PI staining (Figure 7). Even though control cells show some cell death, the CML CD34+ cells are more sensitive, with a marked decrease in proliferation and an increase in the sub-G0/G1 population (20% in control to 60% at 6 nM), whereas control CD34+ cells show a smaller effect (30% cell death at 6 nM). This result confirms that Bcr-Abl1-expressing cells are more sensitive to the proteasome inhibitor Btz.

Discussion

In this report, we have explored the possibility of inhibiting the proteasome in the treatment of CML and analyzed the changes induced by Btz on the molecular mechanisms controlling cell proliferation and survival.

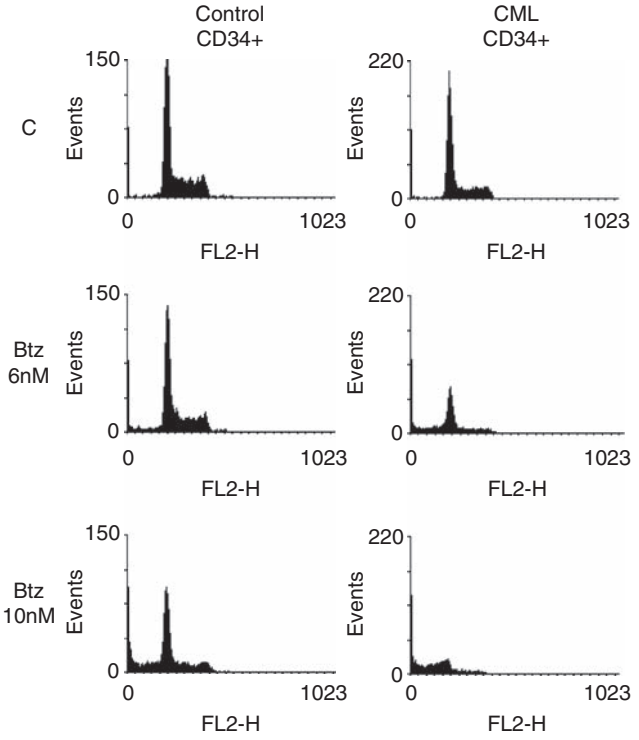

Figure 7 Btz induces cell death in primary CD34+ cells from a CML patient. Control CD34+ cells from umbilical cord (Control CD34+, left) and CD34+ cells from a CML patient (CML CD34+, right) were seeded at 1×10^6 cells/ml and treated with 6 and 10 nM Btz or untreated (C). After 48 h, cells were stained with PI and the cell-cycle profile was analyzed by flow cytometry.

Our results show that Btz induces a cell-cycle arrest and also apoptosis in Bcr-Abl1-expressing cells and not in control cells. The event of apoptosis can be partially prevented with the pan-caspase inhibitor z-VAD indicating the implication of caspases in Btz induced apoptosis in the cell models we have used. Regarding the effect of Btz on proliferation, this inhibitor blocks entry into S phase. This is not only shown by our cell-cycle analysis, but also by preventing apoptosis with the caspase inhibitor z-VAD: the cells treated with this inhibitor display an absence of cells in S phase, with the accumulation of the cells in G0/G1 and in G2/M. This indicates that the effects of Btz on proliferation and survival can be separated and suggests that the apoptosis could be a consequence of the cell-cycle arrest.

At the molecular level, the effect of Btz is characterized by a decrease in the phosphorylation status and later processing of Rb, the latter being related to the apoptosis induced by Btz. We propose that the G1 cell-cycle arrest induced by the inhibition of the proteasome by Btz is the consequence of a series of events involving the failure in the activation of NF-κB2 with a decrease in the expression of c-Myc and Skp2 that results in the accumulation of p21 and p27, inhibitors of the kinase activity of G1 Cyclin/Cdk complexes. As a result, Rb is not correctly maintained in its phosphorylated form and keeps E2F sequestered and inactive, reducing the expression of CycA and preventing S-phase entry. On the other hand, Btz induces the activity of caspases involved in apoptosis and these proteases are also responsible for the proteolitic cleavage of Rb inactivating the anti-apoptotic function of this protein (Janicke *et al*., 1996).

There are some works reporting that Btz inhibits growth of Bcr-Abl1-expressing cells. Most of them use Btz in combination with other drugs (Yu *et al*., 2003; Dai *et al*., 2004; Dasmahapatra *et al*., 2006; Yan *et al*., 2007) or lack the use of control cells (Gatto *et al*., 2003). In our case, we have used Btz alone at a dose that has no effect on BaF/3 cells that do not express Bcr-Abl1, showing that Btz alone is sufficient to arrest the cell cycle and induce apoptosis specifically in Bcr-Abl1-expressing cells. The use of control cells reinforces the idea of the higher sensitivity of tumor cells to the inhibition of the proteasome (Joazeiro *et al*., 2006; Vink *et al*., 2006). We also show that Btz is able to induce the same effects on cells expressing mutant forms of Bcr-Abl1 that confer resistance to IM. These effects are indistinguishable from the ones seen with IM-sensitive Bcr-Abl1-expressing cells. Moreover, Btz is able to induce apoptosis also in the kinase inhibitor-resistant mutant T315I.

We also show that Btz is effective in primary CD34+ cells from a CML patient. Very recently, Heaney and co-workers have also shown that Btz induces apoptosis of primary CD34+ cells and also the more primitive CD34+38-cells from CML patients. These authors show that Btz reduces (1) the capacity of these cells to form colonies in long-term cultures and (2) the engraftment potential of these human CD34+ CML cells (Heaney *et al*., 2010). This indicates that Btz can target CML stem cells that are resistant to IM treatment.

NF-κB is commonly inactive in Btz-treated cells (Adams, 2001; Sartore-Bianchi *et al*., 2007; Galimberti *et al*., 2008; Markovina *et al*., 2008; Ocio *et al*., 2008; Yang *et al*., 2008). In our case, Btz reduces the DNA-binding activity of NF-κB in control and Bcr-Abl1-expressing cells. Therefore, this protein does not seem to be responsible for the effects we see only in Bcr-Abl1-expressing cells. However, there is a difference in the effect of Btz on the activation of NF-κB2 that could be responsible for the cell-cycle arrest and, perhaps, also the caspase-dependent apoptosis that we observe. We show the inactivation of NF-κB2 by Btz in a direct way, by measuring the level of processing from the inactive 100 kDa form to the active 52 kDa form, and also indirectly, by analyzing the expression levels of two known targets of NF-κB2, namely Skp2 and c-Myc. This result establishes a new link between Bcr-Abl1 and the NF-κB2 signaling pathway that is sensitive to proteasome inhibition in CML cells.

In summary, this work shows that Btz reduces the proliferation and survival of Bcr-Abl1-expressing cells, regardless of their sensitivity to IM and including the highly resistant mutant T315I. Our results also show that the inhibition of the proteasome affects the Rb pathway through the inactivation of NF-κB2. This, in

turn, reduces the level of Skp2 and c-Myc. The central functions of these two potent oncoproteins in regulating the cell cycle indicates that Btz is affecting important pathways that are usually altered in tumor cells, suggesting that this drug could have potential uses not only in CML but also in other types of tumors.

Materials and methods

Cell culture

BaF/3 control cells, Bcr-Abl1-expressing BaF/3-p210 cells, and BaF/3 cells expressing IM-resistant Bcr-Abl1 mutants were a kind gift of Dr Druker (Griswold *et al*., 2006). The TCC-S cell line derived from a CML patient in blast crisis and that expresses mainly the p210 form of Bcr-Abl1 and, to a lower extent, also the p190 form of the oncoprotein (Van *et al*., 2005) was obtained from the American Type Culture Collection (Manassas, VA, USA). These cell lines were grown in RPMI supplemented with 10% FCS, L-glutamine, and penicillin streptomycin. In the case of the BaF/3 cells, 10% WEHI-conditioned medium was added to the culture medium as a source of murine IL-3, whereas growth of Bcr-Abl1-expressing BaF/3 cells was independent of growth factors. Primary CML CD34+ cells and control CD34+ cells from umbilical cord blood, obtained after informed consent, were selected and cultured as described (Andreu *et al*., 2005). All media, serum, and supplements were from Invitrogen Life Technologies (Paisley, UK). When indicated, cell lines were treated with the tyrosine-kinase inhibitor IM (STI571, Gleevec, generously provided by Dr Elisabeth Buchdunger, Novartis, Basel, Switzerland). The reversible proteasome inhibitor Btz (PS341, Velcade) was kindly supplied by Millenium Pharmaceuticals (Cambridge, MA, USA). Both drugs were administered as a single dose at the beginning of the experiment. To inhibit caspase activity, cells were pre-treated for 1 h with 100 μM of the pan-caspase inhibitor z-Val-Ala-DL-Asp(OMe)-fluoromethylketone (z-VAD) (Bachem, Bubendorf, Switzerland). Cell lines were seeded at a density of 1×10^5/ml and viable cells (assessed by Trypan blue exclusion) were counted at different time points as indicated.

Analysis of the cell cycle and apoptosis by flow cytometry

Cell-cycle profiles were obtained by PI staining using the DNA Prep Reagent System (Beckman Coulter, Fullerton, CA, USA). Briefly, 5×10^5 cells were washed twice in cold PBS, fixed in ice-cold 80% ethanol and kept at −20 °C until further analyzed. For a detailed analysis of the cell-cycle distribution, cells were labeled for 30 min with 0.5 μM of the nucleotide analog EdU using the Click-iT EdU Flow Cytometry Assay (Invitrogen, Eugene, OR, USA) following the manufacturer's instructions. The double staining with EdU and PI allows the quantification of the cell populations in the G0/G1, S, and G2/M phases of the cell cycle. Phosphatidylserine exposure was used as an indication of apoptosis and quantified by Annexin-V/PI staining with Annexin-V-FLUOS Stainning kit (Roche, Mannheim, Germany). PI staining of un-fixed cells to quantify the sub-G0/G1 population was also used as a measure of apoptosis. Cells were analyzed in a FC500 flow cytometer (Beckman Coulter), using CytomicsTM RXP and WinMDI programs.

Western blot analysis

For analysis of protein expression, cell extracts were prepared and analyzed as earlier described (Poch *et al*., 2007). We used primary antibodies against the following proteins: p27Kip1 (C19 and F8), p21Cip1 (C19), c-Myc (N262), CycA (C19), and NF-κB2 (k27) from Santa Cruz Biotechnology (Santa Cruz, CA, USA); p45Skp2 (2B12) from Zymed (San Francisco, CA, USA); Rb (G3-245) from BD Biosciences-Pharmingen (San Jose, CA, USA); and β-tubulin from Sigma (St Louis, MO, USA). Horseradish peroxidase-conjugated secondary antibodies were from Pierce (Rock-Ford, IL, USA). Blots were developed using the enhanced chemiluminescence system (ECL Plus, Amersham Bioscience, Little Chalfont, UK). Rb phosphorylation was analyzed as described earlier (Andreu *et al*., 2005). Samples were separated in $20 \times 20\,cm^2$ PAGE gels. We used the QuantityOne software (Bio-Rad, Hercules, CA, USA) to quantify the intensity of the bands.

Electrophoretic mobility shift assay

To obtain nuclear extracts, 10×10^6 cells were collected, washed in PBS, and centrifuged at 500 *g* at 4 °C. The pellet was resuspended in cytosol extraction buffer containing 5 mM Na_2HPO_4 pH 7.4, 50 mM NaCl, 150 mM sucrose, 5 mM KCl, 2 mM DTT, 1 mM MgCl2, 0.5 mM $CaCl_2$, and 0.1 mM PMSF (phenylmethylsulphonyl fluoride) with 0.1% NP-40, were left on ice for 3 min, and centrifuged at 1000 *g*, 10 min at 4 °C in a refrigerated Eppendorf 5417 R centrifuge with a fixed angle rotor. The pellet was gently resuspended again in the same buffer without NP-40 and deposited on a solution containing 30% sucrose, 2.5 mM Tris–HCl pH 7.4, and 10 mM NaCl, prepared fresh for each sample and centrifuged at 1000 *g*, 10 min at 4 °C. The pellet was resuspended in nuclear extraction buffer (50 mM Tris–HCl pH 7.4, 300 mM NaCl, and 0.5% Triton X-100). Once resuspended, the samples were incubated on ice 20–30 min, subsequently centrifuged at 10 000 *g*, 10 min at 4 °C, and the supernatant corresponding to the nuclear fraction was collected and quantified with the DC protein assay (Bio-Rad). The DNA-binding activity of NF-κB in these extracts was analyzed by electrophoretic mobility shift assay using the DIG Gel Shift Kit, Second Generation (Roche) and following the manufacturer's instructions. The nuclear extracts (10 μg) were incubated with Digoxigenin-labeled double-stranded DNA oligonucleotides corresponding to the consensus-binding site for NF-κB 5′-AG TTGAGGGGACTTTCCCAGGC-3′ (Dai *et al*., 2004).

Statistical analysis

Microsoft Excel and GraphPadPrism were used to analyze the data and calculate IC_{50} values from dose-response plots. To analyze the possible synergism between IM and Btz on BaF/3-p210 cells, we used the CalcuSyn software (Biosoft, Cambridge, UK) based on the Chou and Talalay method (Chou and Talalay, 1984).

Conflict of interest

The authors declare no conflict of interest.

Acknowledgements

We thank Dr Elisabeth Buchdunger at Novartis for providing us with Imatinib and Millenium Pharmaceuticals for the kind gift of Bortezomib. We also thank Dr BJ Druker for the mutant Bcr-Abl1-expressing BaF/3 cells. The study was supported by grants from the Instituto de Salud Carlos III PI060285, PI070602 and RD06/0020 to IPR, FP and EJA; from the Consellería de Sanitat to IPR; from the Cardenal

Herrera-CEU University (PRUCH and Santander-Copernicus) to IPR and 'UTE project CIMA'. Fellowships were from the Cardenal Herrera-CEU University to MPA and JJV and from the Generalitat Valenciana to JMV. EJA is supported by the program Ramon y Cajal from the Ministerio de Ciencia e Innovación.

References

Adams J. (2001). Proteasome inhibition in cancer: development of PS-341. *Semin Oncol* **28**: 613–619.

Andreu EJ, Lledo E, Poch E, Ivorra C, Albero MP, Martinez-Climent JA *et al*. (2005). BCR-ABL induces the expression of Skp2 through the PI3K pathway to promote p27Kip1 degradation and proliferation of chronic myelogenous leukemia cells. *Cancer Res* **65**: 3264–3272.

Barre B, Perkins ND. (2007). A cell cycle regulatory network controlling NF-kappaB subunit activity and function. *EMBO J* **26**: 4841–4855.

Brignole C, Marimpietri D, Pastorino F, Nico B, Di Paolo D, Cioni M *et al*. (2006). Effect of bortezomib on human neuroblastoma cell growth, apoptosis, and angiogenesis. *J Natl Cancer Inst* **98**: 1142–1157.

Chauhan D, Bianchi G, Anderson KC. (2008). Targeting the UPS as therapy in multiple myeloma. *BMC Biochem* **9**(Suppl 1): S1.

Chou TC, Talalay P. (1984). Quantitative analysis of dose-effect relationships: the combined effects of multiple drugs or enzyme inhibitors. *Adv Enzyme Regul* **22**: 27–55.

Crawford LJ, Windrum P, Magill L, Melo JV, McCallum L, McMullin MF *et al*. (2009). Proteasome proteolytic profile is linked to Bcr-Abl expression. *Exp Hematol* **37**: 357–366.

Dai Y, Rahmani M, Pei XY, Dent P, Grant S. (2004). Bortezomib and flavopiridol interact synergistically to induce apoptosis in chronic myeloid leukemia cells resistant to imatinib mesylate through both Bcr/Abl-dependent and -independent mechanisms. *Blood* **104**: 509–518.

Dasmahapatra G, Nguyen TK, Dent P, Grant S. (2006). Adaphostin and bortezomib induce oxidative injury and apoptosis in imatinib mesylate-resistant hematopoietic cells expressing mutant forms of Bcr/Abl. *Leuk Res* **30**: 1263–1272.

Druker BJ. (2008). Translation of the Philadelphia chromosome into therapy for CML. *Blood* **112**: 4808–4817.

Galimberti S, Canestraro M, Pacini S, Fazzi R, Orciuolo E, Trombi L *et al*. (2008). PS-341 (Bortezomib) inhibits proliferation and induces apoptosis of megakaryoblastic MO7-e cells. *Leuk Res* **32**: 103–112.

Gatto S, Scappini B, Pham L, Onida F, Milella M, Ball G *et al*. (2003). The proteasome inhibitor PS-341 inhibits growth and induces apoptosis in Bcr/Abl-positive cell lines sensitive and resistant to imatinib mesylate. *Haematologica* **88**: 853–863.

Griswold IJ, Macpartlin M, Bumm T, Goss VL, O'Hare T, Lee KA *et al*. (2006). Kinase domain mutants of Bcr-Abl exhibit altered transformation potency, kinase activity, and substrate utilization, irrespective of sensitivity to imatinib. *Mol Cell Biol* **26**: 6082–6093.

Heaney NB, Pellicano F, Zhang B, Crawford L, Chu S, Kazmi SM *et al*. (2010). Bortezomib induces apoptosis in primitive chronic myeloid leukemia cells including LTC-IC and NOD/SCID repopulating cells. *Blood* (e-pub ahead of print 12 January 2010; doi:10.1182/blood-2008-06-164582).

Heusch M, Lin L, Geleziunas R, Greene WC. (1999). The generation of nfkb2 p52: mechanism and efficiency. *Oncogene* **18**: 6201–6208.

Janicke RU, Walker PA, Lin XY, Porter AG. (1996). Specific cleavage of the retinoblastoma protein by an ICE-like protease in apoptosis. *EMBO J* **15**: 6969–6978.

Joazeiro CA, Anderson KC, Hunter T. (2006). Proteasome inhibitor drugs on the rise. *Cancer Res* **66**: 7840–7842.

Kano Y, Akutsu M, Tsunoda S, Izumi T, Kobayashi H, Mano H *et al*. (2007). Cytotoxic effects of histone deacetylase inhibitor FK228 (depsipeptide, formally named FR901228) in combination with conventional anti-leukemia/lymphoma agents against human leukemia/lymphoma cell lines. *Invest New Drugs* **25**: 31–40.

Khidr L, Chen PL. (2006). RB, the conductor that orchestrates life, death and differentiation. *Oncogene* **25**: 5210–5219.

Kossatz U, Dietrich N, Zender L, Buer J, Manns MP, Malek NP. (2004). Skp2-dependent degradation of p27kip1 is essential for cell cycle progression. *Genes Dev* **18**: 2602–2607.

Markovina S, Callander NS, O'Connor SL, Kim J, Werndli JE, Raschko M *et al*. (2008). Bortezomib-resistant nuclear factor-kappaB activity in multiple myeloma cells. *Mol Cancer Res* **6**: 1356–1364.

Murray AW. (2004). Recycling the cell cycle: cyclins revisited. *Cell* **116**: 221–234.

Ocio EM, Mateos MV, Maiso P, Pandiella A, San-Miguel JF. (2008). New drugs in multiple myeloma: mechanisms of action and phase I/II clinical findings. *Lancet Oncol* **9**: 1157–1165.

Perez-Galan P, Roue G, Villamor N, Montserrat E, Campo E, Colomer D. (2006). The proteasome inhibitor bortezomib induces apoptosis in mantle-cell lymphoma through generation of ROS and Noxa activation independent of p53 status. *Blood* **107**: 257–264.

Perez-Roger I, Kim SH, Griffiths B, Sewing A, Land H. (1999). Cyclins D1 and D2 mediate myc-induced proliferation via sequestration of p27(Kip1) and p21(Cip1). *EMBO J* **18**: 5310–5320.

Poch E, Minambres R, Mocholi E, Ivorra C, Perez-Arago A, Guerri C *et al*. (2007). RhoE interferes with Rb inactivation and regulates the proliferation and survival of the U87 human glioblastoma cell line. *Exp Cell Res* **313**: 719–731.

Pomerantz JL, Baltimore D. (2002). Two pathways to NF-kappaB. *Mol Cell* **10**: 693–695.

Ramirez P, DiPersio JF. (2008). Therapy options in imatinib failures. *Oncologist* **13**: 424–434.

Roman-Gomez J, Jimenez-Velasco A, Agirre X, Castillejo JA, Navarro G, San Jose-Eneriz E *et al*. (2007). Epigenetic regulation of human cancer/testis antigen gene, HAGE, in chronic myeloid leukemia. *Haematologica* **92**: 153–162.

Sartore-Bianchi A, Gasparri F, Galvani A, Nici L, Darnowski JW, Barbone D *et al*. (2007). Bortezomib inhibits nuclear factor-kappaB dependent survival and has potent in vivo activity in mesothelioma. *Clin Cancer Res* **13**: 5942–5951.

Sawyers CL. (1993). The role of myc in transformation by BCR-ABL. *Leuk Lymphoma* **11**: 45–46.

Shah NP, Sawyers CL. (2003). Mechanisms of resistance to STI571 in Philadelphia chromosome-associated leukemias. *Oncogene* **22**: 7389–7395.

Sherr CJ, Roberts JM. (2004). Living with or without cyclins and cyclin-dependent kinases. *Genes Dev* **18**: 2699–2711.

Stapnes C, Doskeland AP, Hatfield K, Ersvaer E, Ryningen A, Lorens JB *et al*. (2007). The proteasome inhibitors bortezomib and PR-171 have antiproliferative and proapoptotic effects on primary human acute myeloid leukaemia cells. *Br J Haematol* **136**: 814–828.

Strauss SJ, Higginbottom K, Juliger S, Maharaj L, Allen P, Schenkein D *et al*. (2007). The proteasome inhibitor bortezomib acts independently of p53 and induces cell death via apoptosis and mitotic catastrophe in B-cell lymphoma cell lines. *Cancer Res* **67**: 2783–2790.

Van PN, Xinh PT, Kano Y, Tokunaga K, Sato Y. (2005). Establishment and characterization of a novel Philadelphia-chromosome positive chronic myeloid leukemia cell line, TCC-S, expressing P210 and P190 BCR/ABL transcripts but missing normal ABL gene. *Hum Cell* **18**: 25–33.

Vink J, Cloos J, Kaspers GJ. (2006). Proteasome inhibition as novel treatment strategy in leukaemia. *Br J Haematol* **134**: 253–262.

Wei AH, Roberts AW. (2008). Bortezomib: putting mantle cell lymphoma on death row. *Leuk Lymphoma* **49**: 657–658.

Yan H, Wang YC, Li D, Wang Y, Liu W, Wu YL *et al*. (2007). Arsenic trioxide and proteasome inhibitor bortezomib synergistically induce apoptosis in leukemic cells: the role of protein kinase Cdelta. *Leukemia* **21**: 1488–1495.

Yang DT, Young KH, Kahl BS, Markovina S, Miyamoto S. (2008). Prevalence of bortezomib-resistant constitutive NF-kappaB activity in mantle cell lymphoma. *Mol Cancer* **7**: 40.

Yu C, Rahmani M, Conrad D, Subler M, Dent P, Grant S. (2003). The proteasome inhibitor bortezomib interacts synergistically with histone deacetylase inhibitors to induce apoptosis in Bcr/Abl+ cells sensitive and resistant to STI571. *Blood* **102**: 3765–3774.

Zhao X, Qiu W, Kung J, Peng X, Yegappan M, Yen-Lieberman B *et al*. (2008). Bortezomib induces caspase-dependent apoptosis in Hodgkin lymphoma cell lines and is associated with reduced c-FLIP expression: a gene expression profiling study with implications for potential combination therapies. *Leuk Res* **32**: 275–285.